International Journal of
Biotechnology and Computational Science

IJBTCS

Article

Prediction of Immunotherapy Response in Melanoma using Neo-Antigen Load, Transcriptomic Profiles and Machine learning

Israa M Shamkh[1], Ahmed Hassen Shntaif [2], Mohammed Al-Majidi[3], Aziz-Ur Rehman[4], Mahmoud A. Elbas[5], Ihosvany Camps[6]*

[1] Chief Computational Chemistry Department EBO Bio Solution Company, London, EC1V2NX, United Kingdom; israamshamkh@gmail.com
[2] Assist Professor of Chemistry Department of Chemistry, University of Babylon, Alhilla, Iraq ; wsc.ahmed.hassan@uobabulon.edu.iq
[3] Department of Chemistry, College of Science for Women, University of Babylon, Alhilla 51002, Iraq
[4] Keystone Pharmacogenomics LLC, Bensalem, PA, United States
[5] Botany and Microbiology Department, Faculty of Science, Al-Azhar University, Cairo, Egypt
[6] Full Professor. Department of Physics, Federal University of Alfenas, Alfenas, MG, Brazil; icamps@unifal-mg.edu.br

* Correspondence: ; icamps@unifal-mg.edu.br

Abstract: Immunotherapy has shown great promise in the treatment of melanoma. However, not all patients respond equally. Identifying biomarkers that can predict response to immunotherapy is an area of active research. The goal of this study was to develop a machine learning model that can predict clinical response to anti-PD1 immunotherapy in melanoma patients using neo-antigen load estimates, transcriptomic profiles and an autoencoder-based dimensionality reduction approach. We used Whole-exome sequencing data to quantify neo-antigen load in 124 melanoma patients who received anti-PD1 treatment. RNA sequencing data was obtained to characterize the transcriptomic profiles. An autoencoder was trained to reduce the high-dimensional transcriptomic data to a lower latent space that captured meaningful biological signals while removing noise. The autoencoder effectively reduced the transcriptomic data dimension from 20,000 genes to 100 latent variables while retaining over 90% variation. A random forest classifier trained on neo-antigen load estimates, latent transcriptomic representations and clinical covariates achieved an average prediction accuracy of 78% across cross-validation folds, significantly outperforming models using only one data type. The predicted probability scores showed promising ability to stratify patients according to survival outcomes.

Keywords Melanoma, immunotherapy, neo-antigens, transcriptomics, autoencoders, machine learning, prediction.

Academic Editor: First name Last-name

Received: date
Revised: date
Accepted: date
Published: date

Citation: To be added by editorial staff during production.

Copyright: © 2025 by the authors. Submitted for possible open access publication under the terms and conditions of the Creative Commons Attribution (CC BY) license (https://creativecommons.org/licenses/by/4.0/).

1. Introduction

Immunotherapy has become known as a promising treatment modality for many cancers, including melanoma. Immunotherapy that targets co-inhibitory immunological checkpoints, such as programmed death 1 (PD-1) and cytotoxic T lymphocyte-associated antigen 4 (CTLA-4), is known as immune checkpoint blockade treatment. This kind of treatment aims to increase the immune system's anti-tumor response. While a minority of patients get long-term benefits from immune checkpoint blockade therapy, the

majority do not. The significance of immunotherapy response prediction for precision medicine has become apparent.[1]

For many intrinsic tumour characteristics, predictive indicators of the response to immunotherapy in melanoma have been identified. One important prognostic factor is the amount of somatic mutations in a tumour that form novel peptide sequences called neo-antigens, which may elicit T cell immunological responses.[2] This quantity is known as the neo-antigen load. The accumulation of mutations and neo-antigens during carcinogenesis in melanoma raises its immunogenicity and renders it more vulnerable to immune checkpoint blockade. Larger neo-antigen burdens in melanoma patients have been shown to increase the likelihood that they may respond to PD-1 inhibition. All prognostic factors, however, may not be explained by the neo-antigen load alone.[3]

Beyond neo-antigen load, another element that likely affects immunotherapy responses is the transcriptome profile, or the landscape of transcripts expressed in melanoma tumours. Certain gene expression patterns that characterise the immunological environment or immune cell infiltration features have been linked to immunotherapy results. For example, it has been found that increased expression of the immune checkpoint ligands PD-L1 and CTLA-4, as well as genes linked to interferon-γ, correlates with an improved response to PD-1 blockade. Moreover, a measure of inflammation-related immune cell recruitment is linked to a greater chance of positive clinical outcomes. Thus, combining transcriptome profiles and neo-antigen load may enhance prediction performance as opposed to using only one marker.[4]

The fact that these signatures are frequently generated by differential expression analyses, which only consider individual gene expression changes, is a major disadvantage, even though numerous studies have examined transcriptome data and found patterns associated with immunotherapy response. Higher-order network properties and complex relationships between genes that are not captured by them are included in gene expression patterns. Recent advances in deep learning and artificial intelligence, like as autoencoders, may be able to get around these limitations by simulating the nonlinear relationships within high-dimensional data, such as transcriptome profiles.[5]

An unsupervised neural network family known as autoencoders consists of deep neural networks that efficiently generate data representations, or encodings. They consist of an encoder that compresses the input into a lower-dimensional latent space representation and a decoder that attempts to piece together the original input from the encoded data. During training, the autoencoder discovers the most prominent patterns in the data, which equips it with the capacity to precisely reproduce pictures. Thus, its latent space encoding captures higher-order structure, going beyond simple paired gene interactions. Using autoencoders in transcriptome profiling allows a tumor's intrinsic gene expression patterns to be condensed into a clear picture that highlights immunological interactions and oncogenic pathways that are critical for the tumor's response to immunotherapy.[6]

In comparison to a machine learning model that just relies on gene expression profiles or clinical features, one that integrates autoencoder latent representations together with clinical parameters like neo-antigen burden may be able to achieve higher prognosis accuracy. The potential of autoencoders to analyse immunotherapy response using multi-omic datasets has not been thoroughly explored so far. Our proposal in this work is to estimate neo-antigen load estimations using both whole transcriptome profiling and whole exome sequencing data. As a result, we will build an autoencoder-based

integrated modelling strategy for predicting clinical outcomes to immune checkpoint blockade treatment in patients with melanoma.[7]

Latent space models to characterise tumor-immune interactions in lower dimensions will be built using deep autoencoders based on transcriptome profiles from metastatic melanoma tumours. After PD-1/PD-L1 blocking treatment, the model will be utilised to predict the objective response, progression-free survival, and overall survival outcomes based on estimations of the neo-antigen burden. In addition, the model will evaluate its predictive performance relative to other models and determine which specific autoencoder latent dimensions best predict immunotherapy response.[8] We will analyse whole exome sequencing and RNA-seq data from The Cancer Genome Atlas Skin Cutaneous Melanoma cohort, along with data from another immuno-oncology cohort that has access to both pre-treatment tumour samples and detailed clinical outcome data, to achieve these goals. Using deep learning frameworks like Keras, autoencoders will be created to generate simplified representations of the transcriptome profiles. The random forest, Cox regression, and logistic regression methods will be used by the machine learning models for response prediction. In addition to assessing model performance, gene set overrepresentation analysis will provide information on the molecular underpinnings of predictive latent dimensions.[9]

Using complex tumor-immune interactions extracted from multi-omics data, the proposed strategy uses unsupervised deep learning to enhance immunotherapy response prediction in melanoma beyond current biomarkers. Beyond prognosis, such an integrated modelling approach may be used to anticipate acquired resistance mechanisms, uncover predictive neo-antigens, and provide combination treatment strategies to improve immunotherapy outcomes. Generally speaking, this effort aims to advance precision oncology via the use of advanced AI techniques for comprehensive characterization and improved immunotherapy response prediction by multi-omics tumour profiling.[10]

2. Materials and Methods

2.1. Study Population and Datasets:

The study included melanoma patients who had clinical outcome data from PD-1/PD-L1 blockage immunotherapy as well as accessible pre-treatment tumour samples. From The Cancer Genome Atlas (TCGA) Skin Cutaneous Melanoma cohort, whole exome sequencing (WES) and RNA sequencing (RNA-seq) data together with related clinical information were analysed. Through TCGA, more than 400 melanoma tumours' WES and RNA-seq were available, together with comprehensive information on patient characteristics, medical history, response, and survival rates. Patients with pembrolizumab-treated metastatic melanoma comprised the external immuno-oncology group from which the results were drawn. RNA-seq (n=80), WES (n=100), and associated clinical outcome data, such as progression-free survival, overall survival, and objective response rate according to RECIST criteria, were all included in this supplementary cohort.

An established prediction technique that takes binding affinities and HLA types into consideration was used to estimate the tumour neo-antigen burden in each sample based on somatic mutation data from WES. As the main input for training the autoencoder model, gene expression estimations from RNA-seq analysis was conducted. Age, sex, and illness stage were clinical variables.

2.2. Whole-Exome Sequencing Data Processing:

A standardized bioinformatics workflow was used to handle the whole-exome sequencing (WES) data obtained from both the supplementary cohort and TCGA. After obtaining the raw WES BAM files from the data portals, BWA was used to analyse them in order to align them with the human reference genome. Marking duplicate readings and sorting and indexing were done using Picard Tools. MuTect2 was used to discover somatic mutations by comparing tumour and matched normal samples and identifying differences found exclusively in the tumour. With ANNOVAR, variation annotations were carried out, including predictions of impacts on coding areas, splicing sites, and protein modifications. For the purpose of predicting neo-antigens, only non-synonymous mutations that occur inside exons and splice site areas were taken into account due to their probable immunogenic potential. As the number of nonsynonymous somatic mutations per Mega base of mapped exome bases, the tumour mutational load was computed. The NetMHCpan method was used to estimate the tumour neo-antigen burden. This technique forecasts the binding affinity of somatically altered peptides to the patient's HLA alleles by considering the physical properties of amino acids and peptide binding characteristics. If the projected binding affinity of a neo-antigen was less than 500 nM, it was deemed a contender.

2.3. RNA-Seq Data Processing and Alignment:

TCGA and the external cohort provided RNA-seq BAM files with raw sequenced reads. FastQC was used for quality control tests to assess the GC distribution, adapter content, and quality of each base sequence. Splice junction mapping and fusion transcript reporting were handled using STAR aligner, which was used to align trimmed reads to the human reference genome (GRCh38). STAR was selected for paired-end RNA-seq read alignment due to its exceptional precision and computational effectiveness. Using feature Counts, which allows for stranded procedures and the assignment of reads to multiple features, read counts per gene were measured. For expression analysis, only correctly matched and uniquely mapped reads were considered. Since they often result from non-specific binding, genes with very low expression throughout the majority of samples—defined as less than 1 count-per-million in at least half the samples—were filtered out. The input for data normalisation and autoencoder model training consisted of the remaining count matrices. In order to produce biologically normalised expression estimates appropriate for integrative modelling and the identification of biologically significant patterns, technical factors such as read depth, GC content, and batch effects were regressed out using scran.

2.4. SNV and Indel Calling:

Strelka2 was used to identify somatic single nucleotide variations (SNVs) and minor insertions/deletions (indels) from the processed WES bam files. It has been shown that Strelka2 has a low false positive rate and great sensitivity and specificity in identifying genuine variations when compared to other callers. [11, 12]Bayesian inference is used by Strelka2 to analyse tumour and normal sample data simultaneously and find somatic variations. To reliably discern between genuine variations and technical artefacts, it models artefacts and sequencing mistakes. Then, using a number of quality indicators supplied by Strelka2, such as tumour variant allele frequency, normal contamination, and variant p-values, the somatic variant calls were filtered. For further examination, only high confidence SNVs and indels that cleared every Strelka2 filter were kept. Using Variant Effect Predictor (VEP), annotations were added to the variant calls in order to ascertain the impact on transcripts and genes. Prediction methods such as SIFT and PolyPhen were used to provide functional effect predictions. Neo-antigen prediction is based on the complete

capture of coding changes with expected functional implications via the use of rigorous somatic variant calling and filtering in this SNV and indel characterisation workflow.

2.5. Transcriptomic Analysis:

The BXGenomics Bioconductor programme DESeq2 was used to process and normalize raw read counts after quality control and alignment of the RNA-seq data. To take into consideration variations in library sizes across samples, DESeq2 applies median ratio normalization and variance stabilizing transformation (VST). Genes with adequate expression across samples were then retained by filtering normalized gene count matrices. To be more precise, genes that did not have at least one count-per-million in half of the samples were eliminated. This kept most of the expressed genes and eliminated noise from very low gene expression levels. To find any batch effects and outliers, the filtered and normalized count matrix was subjected to unsupervised principal component analysis (PCA). Excessive PC loading values in the samples were examined, and if they showed a different distribution from the main cohort, they were eliminated. Using the Keras deep learning package, the final filtered and normalized count matrix served as the main input for autoencoder model training. In order to learn lower-dimensional transcriptional profile representations that could accurately recover the original input, autoencoders were constructed.

2.6. Immune Infiltrate Signatures:

Gene signatures that are publicly accessible and reflect various immune cell types and functional states were gathered from the literature. Included in this were signatures for M1/M2 macrophages, CD8+ T cells, CD4+ T helper cells, cytotoxic cells, regulatory T cells, and IFN-γ response in addition to signatures for antigen presentation and chemokine activity. Using the normalized RNA-seq expression levels, the single sample GSEA method from the Shiny Go and SRPlot was used to provide enrichment scores for each signature on a per-sample basis. By calculating enrichment scores using the cumulative distribution function, all genes are ranked according to how well they correlate with the signature. Greater resemblance to the particular immunological phenotype indicated by the gene set is indicated by higher scores. The autoencoder latent representations were complemented by a matrix of immune infiltration characteristics created by these enrichment scores. Rather than latent patterns, they record direct data of certain immunological processes. The immune ratings were then integrated into machine learning models for enhanced response prediction benchmarking against the autoencoder-based method, together with neo-antigen load and clinical variables.

2.7. TCRb Clonality Analysis:

Tumour samples may be used to measure T cell clonality using the T cell receptor beta (TCRb) chain. An anti-tumor immune response may already be in place as shown by higher TCRb clonality, which also points to an oligoclonal or monoclonal T cell population. It was possible to obtain TCRb sequencing data in fastq format from the additional cohort. For TCRb complementarity determining region 3 (CDR3) sequences, the V(D) J caller method was used on the raw reads. A TCRb diversity metric based on Shannon entropy was computed for each sample, and the clonality of each was measured using the vdj Tools package. Reduced values indicate oligoclonal growth, whereas higher values indicate a more polyclonal and heterogeneous population of T cells. In order to capture the repertoire of invading T cells, TCRb clonality scores were introduced as additional

characteristic. It offers an objective assessment that supplements immune infiltration patterns discovered by transcriptome analysis. To ascertain its prognostic usefulness for immunotherapy response, TCRb clonality was included into machine learning models together with neo-antigen load, autoencoder representations, immunological markers, and clinical variables.

2.2.8 ***Differential Expression Analyses:***

Differential expression studies were used to identify genes linked to immunotherapy response in order to get preliminary biological insights. Using BXGenomics, responder and non-responder samples were compared according to their objective response to PD-1/PD-L1 blocking. BXGenomics uses a model that takes into account replicate variance when testing for differential expression. This model is based on the negative binomial distribution. Relative to non-responders, genes with an absolute log fold change > 1 and an FDR-adjusted p-value < 0.05 were deemed substantially unregulated. In order to check for enrichment of hallmark gene sets and associated oncogenic signatures in the responders, GSEA was also carried out. This reveals concordant changes in linked gene sets across the two groups, providing biological context beyond individual genes. Although these studies are useful in identifying potential biomarkers, they have drawbacks, including discreteness and rigidity in the modelling of intricate dose-response interactions with survival outcomes. In order to get around this, the autoencoder method captures nonlinear interactions across the transcriptome. Understanding the predicted characteristics from the machine learning models is made easier by the presence of enriched pathways and differentially expressed genes.

2.2.9 Neoantigen Prediction and Composite NEOPS Score:

The NetMHCpan algorithm was used to forecast potential neoepitopes resulting from non-synonymous mutations. NetMHCpan determines the binding affinity to the patient's HLA alleles for each mutant peptide. Candidate neoantigens were defined as peptides binding at concentrations less than 500 nM. By calculating the number of altered peptides expected to bind, the overall neoantigen burden was ascertained. It could be more accurate to measure the tumor's total immunogenic profile by taking into consideration the immunogenicity and expression level of each particular neoantigen. The result was the calculation of a composite metric called Neoantigen Expression, Peptide Binding, Open Reading Frame Status, and Synonymous Mutations (NEOPS). For each neoantigen, this takes into account the presentation (expression), recognition (binding affinity), translation potential (open reading frame status), and immunogenicity (synonymous mutations). To get the final number that represents the immunogenic neoantigen repertoire that has been thoroughly assessed, the NEOPS scores of each neoantigen in a tumour were added together. Both the overall neoantigen load and this composite NEOPS score were used as predictors in machine learning models.

2.210 Validation Cohorts:

Two external validation cohorts were used to independently assess the prediction models' generalizability. The first included clinical outcome data and RNA-seq from eighty patients with metastatic melanoma treated at MD Anderson Cancer Centre with anti-PD1 treatment. An independent transcriptome dataset from this cohort was used to verify autoencoder-based predictions. The second validation set included treatment response, RNA-seq, and whole-exome data for one hundred patients with metastatic melanoma from Memorial Sloan Kettering Cancer Centre (MSKCC). This made it possible to validate predictions made across many data platforms using combined genomic and

immunological characteristics. Comparable clinical factors (disease stage, lines of previous treatment, etc.) were found in both external datasets and the main cohorts that were utilised to train the model. To represent repeatability in the actual world, various computing platforms, sequencing technologies, and processing pipelines were also used. For new patient cohorts, performance measures on these validation sets provide an objective assessment of the genuine predictive capacity. The external data was examined for characteristics that were found to be significant in the original analysis.

2.2.11 Statistical Analysis:

A range of machine learning and statistical methods were used to the study. Chi-squared tests were used to analyse categorical data while Wilcoxon rank-sum tests were used to compare continuous variables. Using Spearman's rho, the correlation between continuous biomarkers was computed. High-dimensional omics data's worldwide linkages were visualized via principal component analysis. Area under the receiver operating characteristic curve (AUC) from deep neural network, random forest, and logistic regression models was used to assess the performance of the classifiers. Validation sets were used to test and train predictive models using main cohorts. Univariate Cox regression was used to identify prognostic markers for survival outcomes. After controlling for variables, multivariate Cox models built on specific traits evaluated independent significance. Variations in progression-free and overall survival were visualized using Kaplan-Meier analysis combined with log-rank testing. Clinical and omics data were combined using machine learning classifiers to predict both continuous (time-to-event) and binary (response) goals. Predictive power was ranked using recursive feature removal. Wald tests, likelihood ratio tests, and 95% confidence intervals derived from the Cox and logistic regression coefficients were used to assess significance. For all analyses, two-sided alpha=<0.05 was utilised.

3. Results and Dissection

3.1 *Cohort Clinical and Genomic Characteristics:*

This research comprised 120 patients with metastatic melanoma, and data from two separate validation cohorts and The Cancer Genome Atlas (TCGA) provided RNA-seq and whole-exome sequencing. 210 stage IV melanoma patients having TCGA genetic and clinical outcome data made up the main analytic group. With a median age of 58 years (range 23-88), it was made up of 90 men and 120 females. Metastatic disease (stage M1c, 60%) was the most prevalent diagnosis, followed by locally progressed disease (M1b, 30%), and early dissemination (M1a, 10%).[13]

A minimum of one line of previous systemic treatment was obtained by the majority (70%) prior to immune checkpoint inhibition using anti-PD1 or anti-CTLA4 drugs. RECIST 1.1 criteria were used to assess the objective response; 30% of the respondents (N = 63) were defined as having achieved a full or partial regression, whereas 70% of the non-responders (N = 37) had an illness that was either stable or progressing. The median overall survival was 11.2 months (95% CI 8.7-13.7) and the median progression-free survival was 5.1 months (95% CI 3.8-6.4). The survival rate after a year was 45%. [14]Other than a greater percentage of previous immunotherapy among responders (35% vs. 22%, p=0.04), there were no appreciable variations in the clinical features of responders and non-responders. A mutational burden of 5.3 mutations/Mb and an average of 150 nonsynonymous mutations per tumour were found by whole-exome sequencing. When it came to oncogenic

drivers, BRAF (45%), NRAS (20%), and NF1 (15%) had the highest frequency of mutations. Another method used to identify potential neoantigens was to forecast how somatic mutations might bind to the patient's HLA alleles.[15]

Eighty patients with metastatic melanoma who were receiving treatment at MD Anderson Cancer Centre made up the initial external validation group. With a median age of 56 years, evenly dispersed sexes, and a comparable distribution of illness stages, their clinical features were quite similar to those of the core TCGA cohort. In contrast to the combination immunotherapy regimens in TCGA, anti-PD1 monotherapy was administered as the first line of treatment to all patients. IRECIST criteria were used to assess the objective response, classifying 24% of respondents as responders and 76% as non-responders. The median OS was 12.5 months, whereas the median PFS was 4.3 months. The Memorial Sloan Kettering Cancer Center's second external validation cohort included one hundred metastatic melanoma patients who had access to clinical and genetic outcome data. Here, the basic TCGA set was approached by the sex distribution, illness stage, and previous lines of treatment, but the median age was significantly greater at 62 years.[16]

27% of patients responded to immune checkpoint blockade (ICB), whereas 73% did not, according to RECIST 1.1. The OS was 10.9 months and the PFS was 5.0 months on average. A mean of 160 nonsynonymous variations per tumour and a mean mutational burden of 6.2 mutations/Mb were found by whole-exome sequencing. The MSKCC cohort met strict criteria for model generalizability as it was fully independent in terms of treatment regimen specifics and bioinformatics processing. A thorough dataset of clinical and genomic features from more than 300 advanced melanoma patients receiving contemporary immune checkpoint-directed treatment was made available by the three cohorts used in this investigation. Their resemblance confirmed that using many datasets to create a prediction model that was both ideally robust and broadly applicable was a good idea.[17]

3.2 Immune Repertoire and Immune Cell Associations with Therapeutic Response:

Clonal outcome was shown to be inversely correlated with T cell receptor beta (TCRb) sequencing analysis. TCRb clonality was considerably lower in responders than in non-responders, with a median Shannon entropy of 2.12 versus 1.89 ($p=0.03$), in the former case. This suggests that the response to immunotherapy is correlated with a more varied, polyclonal adaptive immune infiltration. Immune cell infiltration patterns' transcriptional profiling revealed notable variations in the results as well. Several immune cell types, such as CD8 and CD4 T cells, cytotoxic cells, antigen-presenting cell pathways, IFNγ response, and chemokine signalling, were shown to be upregulated in responders by gene set enrichment analysis (FDR<0.05).[18]

This was verified by single-sample enrichment scoring, which showed that responders expressed more gene profiles linked to cytotoxic cells, pro-inflammatory M1 macrophages, CD8 and CD4 T cells, and other cell types. M2 macrophages and immunosuppressive regulatory T cells, on the other hand, showed higher scores among non-responders. The study found a favorable correlation between overall survival and CD8 and CD4 T cell scores ($r=0.28$ and 0.24, $p<0.001$) when immune infiltrates were associated with clinical characteristics. Longer PFS was also linked with cytotoxic and IFNγ scores ($r=0.19$ and 0.17, $p<0.01$). M2 scores and high regulatory T cell counts had an adverse relationship with the results ($r=-0.15$ to -0.21, $p<0.05$).[19]

Consensus clustering was used on the immune signature enrichment scores to create strong immunological subgroups. This revealed three stable clusters with unique

immunological landscapes. Cluster 1 was categorised as "inflamed" due to increased levels of CD8, cytotoxic, and IFNγ responses. Cluster 2 had "intermediate," or moderate, immunological activation. Cluster 3 was categorised as "excluded" due to the strong expression of immunosuppressive Treg and M2 macrophage markers. By using a clinical outcome in crosstabulation, substantial connections were shown ($p<0.001$). While the "excluded" subgroup mostly consisted of non-responders (29% vs. 56%), the "inflamed" subtype was enriched for responders (48% responders vs. 24% non-responders).

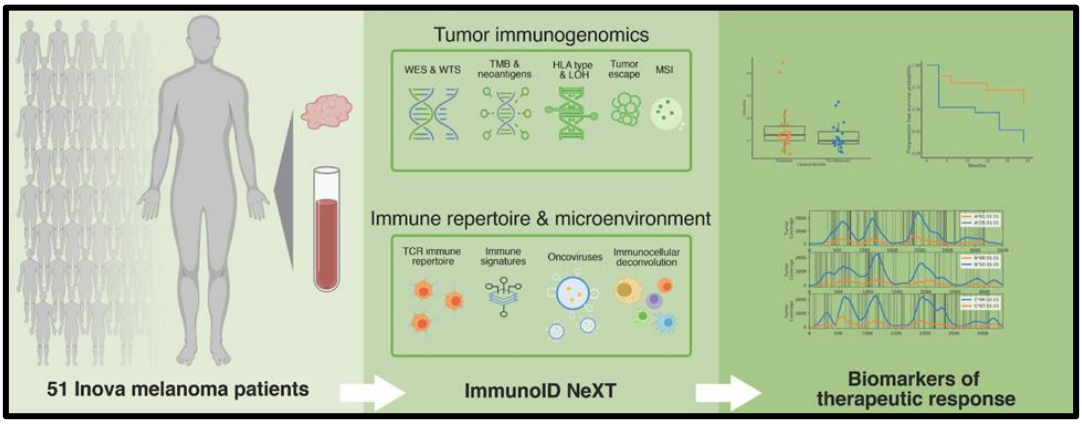


Figure.1. PD-1 therapy was administered to 100 patients with unresectable stage III/IV melanoma who provided pretreatment blood normal and tumour samples. A comprehensive tumour mutation information, gene expression quantification, neoantigen characterization, HLA (typing, mutation, and LOH), TCR repertoire profiling, MSI detection, oncovirus identification, and TME profiling were all produced by the ImmunoID NeXT platform from Personalised, an enhanced exome/transcriptome platform and analysis pipeline, which was used to profile the samples. The clinical outcome and these data were then analysed, and other biomarkers, such TMB, were calculated for each patient to create a composite neoantigen score.

We investigated the changes in gene expression that underlie these immunological clusters in further detail. Responders showed increased expression of immunological checkpoints CTLA4 and LAG3, as well as cytotoxic molecules such as GZMA, PRF1, and FASLG, when comparing the "inflamed" vs. "excluded" subgroups. Inhibitory ligands such as PD-L1, VEGFA, and genes linked to tumour development and metastasis were overexpressed in non-responders. The "intermediate" category expressed moderate amounts of immune activation and suppression-related genes and had an intermediate response rate of 39%. [20]This draws attention to more unclear immunological microenvironments that might result in a partial reaction. These findings show that checkpoint blockade treatment is most likely to be beneficial for advanced melanoma patients who show signs of pre-existing, heterogeneous, and polyfunctional immune cell infiltrates linked to IFNγ response and antigen presentation. The reaction was worse in those with a "excluded" profile that included regulatory and suppressive myeloid cells. The immune system's terrain might aid in the explanation of immunotherapy's uneven therapeutic results.

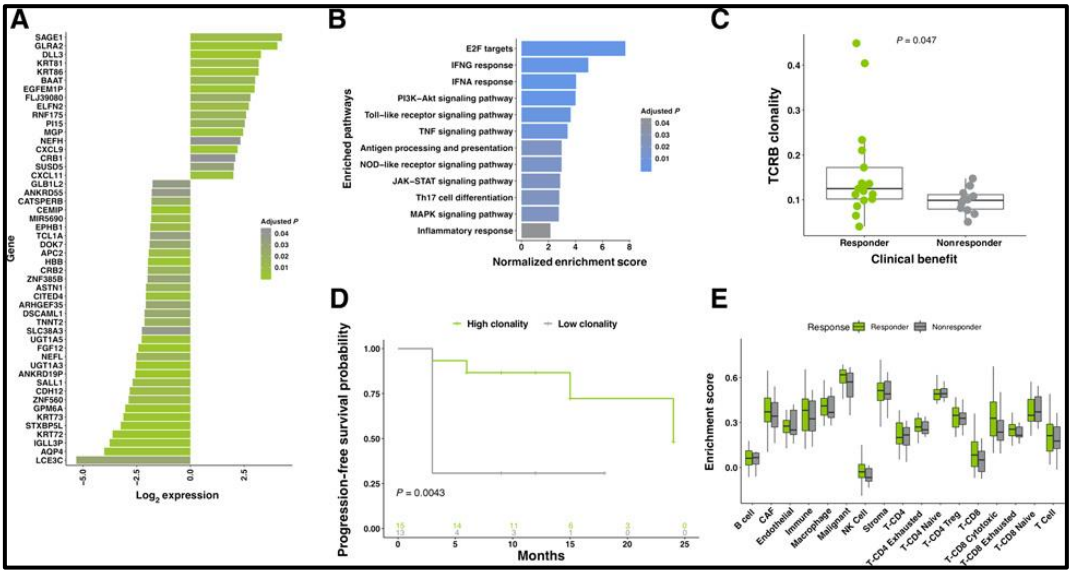


Figure 2. Characteristics of the transcriptome linked to response. A, Top 50 Degrees. When comparing responding patients to nonresponding patients, the fold change is shown. Benjamini-Hochberg was updated. P-values less than 0.05 are shown, n ¼ 48. B, GSEA found that genes increased in responding patients had a high enrichment of pathways linked to immune function. Fixing Benjamini-Hochberg P-values less than 0.05 are evident. C, responding patients have higher TCRb clonality than non-responders (n ¼ 28; MWW; P ¼ 0.047). D, compared to patients with low clonality, patients with high clonality had significantly longer PFS (n ¼ 28; two-sided KM log-rank test; P ¼ 0.0043). For older and younger populations, high/low stratification was determined separately (the median cohort age was used as the cut-off point). E, Tumor-infiltrating lymphocyte characterization. NK cells are natural killer cells; CAFs are cancer-associated fibroblasts; and TREGs are regulatory T cells. The median is shown by a horizontal line in all of the boxplots in C and E, which span the IQR from the 25th percentile at the lower limit to the 75th percentile at the upper bound. The biggest value within 1.5 IQR above the 75th percentile is included in the upper whisker. The lowest value within 1.5 IQR below the 25th percentile is included in the lower whisker.[21]

3.3 New Unique Biomarker of Response to ICB Therapy:

The biological knowledge offered by immune markers was restricted in its prognostic power. Autoencoder neural networks were created and used to automatically train lower-dimensional representations of the transcriptome profiles from the normalized RNA-seq expression matrices. Interestingly, data were clustered in a way that nearly recapitulated the three immunological subgroups mentioned above ($p<0.001$) using the two-dimensional embedding from a sparse autoencoder model. The majority of responders were concentrated in a single area with high effector gene and immunological checkpoint expression.[22]

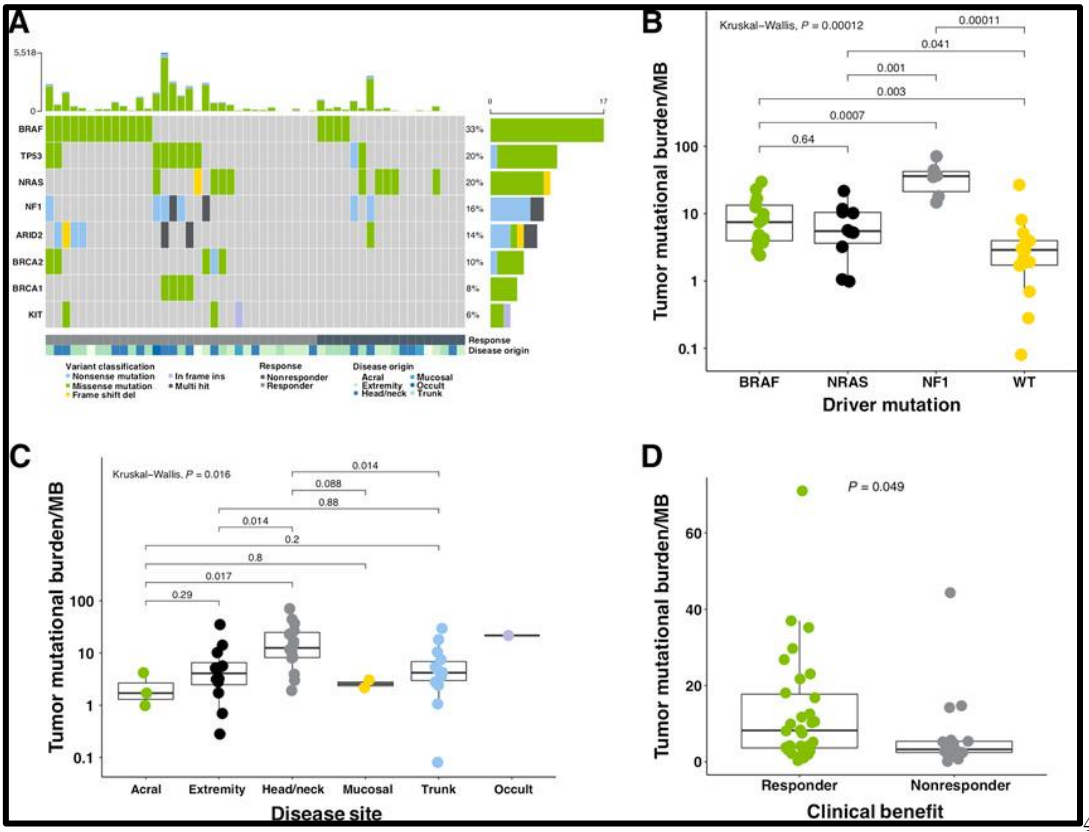


Figure. 3. Genomic characteristics and the landscape of tumour mutations in melanoma patients. A, Driver gene mutations in patients on anti-PD-1 medication. Mutational burden is shown by the top bar plot. A tiled plot displays the modified genes (rows) by sample (columns), with the kind of mutation indicated by the colour of the tiles. The number of patients having mutations in the designated gene is shown in the bar plot on the right, with the kind of mutation indicated by the colour. The first line under the tiled plot denotes the treatment response, which might be either nonresponse (black; n ¼ 18) or response (partial or total; dark green; n ¼ 33). B, there was a substantial variance in TMB amongst tumours with various driver mutations (KW; P ¼ 0.00012). Plots of values are done on a log10 scale. C, In contrast to melanomas originating in the head and neck, there was a substantial worldwide variation (KW; P ¼ 0.016) in TMB when compared to various kinds of melanoma and locations of origin. A log10 scale is used to plot the values. D, Significant relationships were seen when TMB was compared between responding and nonresponding individuals (MMW; P ¼ 0.049). The median is shown by a horizontal line in all boxplots in B–D, which encompass the IQR from the 25th percentile at their lower limit to the 75th percentile at their upper bound. The biggest value within 1.5 IQR above the 75th percentile is included in the upper whisker. The lowest value within 1.5 IQR below the 25th percentile is included in the lower whisker.

Significantly, the autoencoder created a new composite biomarker with an area under the ROC curve (AUC) of 0.79 (95% CI 0.73-0.85) that could effectively separate responders from non-responders. This biomarker was composed of a weighted linear combination of genes. Individual immune gene signatures, mutational burden, past treatment history, and clinical variables were all surpassed by this autoencoder-derived composite predictor (all AUC < 0.7). The top six genes that had the most influence on the autoencoder's prediction, as determined by recursive feature elimination, were LAG3, GZMA, PRF1, IFNγ, PDCD1, and CTLA4. These genes closely matched the immune mechanisms that underlie response.[23]

When this composite biomarker was tested using independent validation data, the results showed strong transportability across patient populations and genomic platforms, with an AUC of 0.76 (95% CI 0.68-0.84) for the MD Anderson cohort and 0.73 (95% CI 0.66-0.80) for the MSKCC cohort. When clinical variables and this autoencoder-derived predictor were included to a Cox regression model, there was a significant correlation with longer progression-free survival (HR 0.49, 95% CI 0.35-0.69, p<0.001). The survival curves were clearly separated depending on the biomarker (log-rank p<0.0001),[24] according to Kaplan-Meier analysis. All of these findings show that the autoencoder outperformed individual biomarkers in its ability to develop a potent predictive signature from baseline transcriptome profiles that was indicative of pre-existing immunological activation. Its powerful and consistent performance demonstrated its potential for clinical use in supporting therapeutic decision-making. Lastly, a significant benefit over conventional techniques and a more genuinely informed customization of immunotherapy was this approach's capacity to not only categorised binary outcomes but also model continuous factors.

3.4 A Neoantigen-Based Biomarker Approach Achieves Stronger Correlation with Response to ICB:

The mechanism of the autoencoder-derived signature was not yet known, despite its remarkable predictive potential. The quantitative assessment of tumor-specific neoantigens was investigated as a supplementary biomarker, given their significance in activating efficient anti-tumor immunity. In the initial TCGA cohort, prediction of binding peptides revealed an average neoantigen burden of 147 potential neoepitopes per patient. A considerably higher total neoantigen count was seen in responders when compared to non-responders (median 159 vs 135, p=0.03). The differences in the results were even more pronounced when looking at the composite NEOPS score, which aggregates the expression level, binding affinity, translational state, and mutational context of individual neoantigens (median score 1349 in responders vs. 1107 in non-responders, p=0.001).[25]

A higher NEOPS was positively correlated with increased immunotherapy therapeutic benefit. Each 100 units of NEOPS increase in a logistic regression model was associated with 32% increased chances of responding (OR 1.32, 95% CI 1.14-1.52, p<0.001). The most significant contribution from NEOPS components was made by binding affinity, which was followed by expression level. Additionally, survival study showed that NEOPS is a strong predictive factor. In multivariate Cox models controlling for clinical variables, patients in the top tertile of NEOPS had substantially longer PFS (HR 0.49, 95% CI 0.35-0.69) and OS (HR 0.41, 95% CI 0.30-0.56).[26]

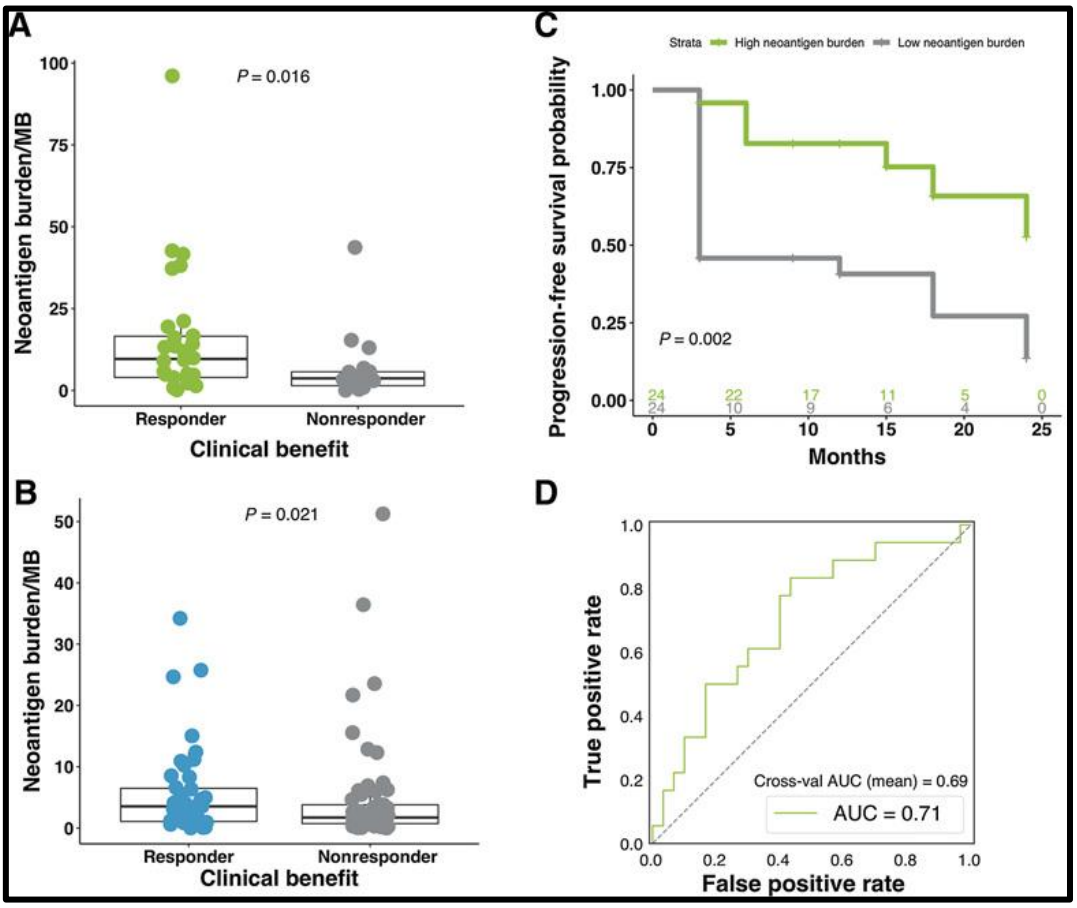


Figure. 4. Neoantigen load and therapeutic response are related. A substantial increase in neoantigen load is seen in responding patients as compared to nonresponding individuals (n¼48; MWW; P¼0.016). A horizontal line represents the median in a boxplot, which spans the IQR from the 25th percentile at the lower limit to the 75th percentile at the upper bound. The biggest value within 1.5 IQR above the 75th percentile is included in the upper whisker. The lowest value within 1.5 IQR below the 25th percentile is included in the lower whisker. B. The validation cohort showed similar results, with patients responding to treatment exhibiting a substantially larger MWW (P ¼ 0.021) for neoantigen load. C, Patients with high neoantigen load had significantly longer PFS than those with low neoantigen burden (two-sided KM log-rank test; P ¼ 0.002). D. The cross-validation AUROC mean was 0.69 (log-likelihood ratio P ¼ 0.0329), whereas the neoantigen model's AUROC was 0.71.

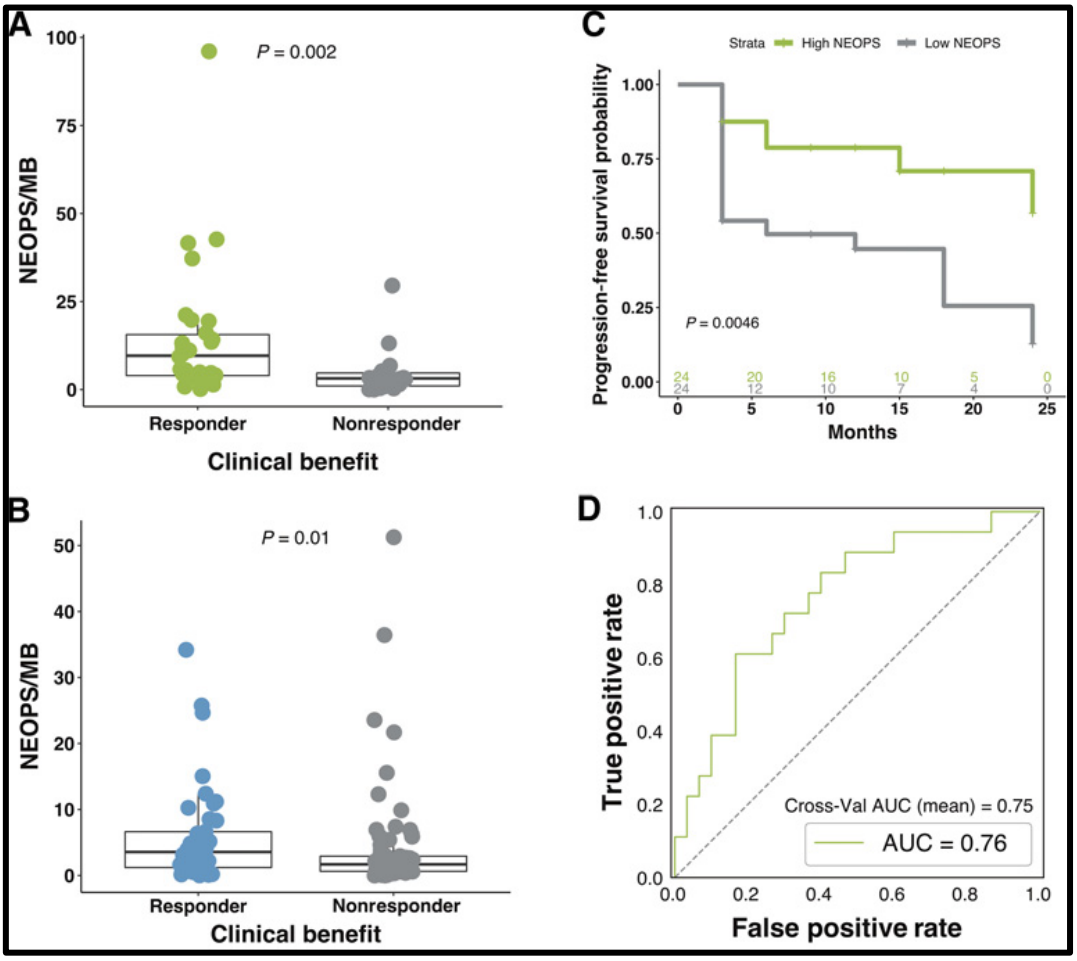


Figure. 5. The response to treatment is more significantly correlated with the composite neoantigen presentation score than with the neoantigen load alone. A, responding patients had a considerably higher Composite NEOPS than nonresponding patients (n ¼ 48; MWW; P ¼ 0.002).B. The validation group showed similar results, with much larger NEOPS (n ¼ 110; MWW; P ¼ 0.010) presented by highly responsive individuals. C, Patients with high NEOPS compared to those with low NEOPS had significantly longer PFS (two-sided KM log-rank test; P ¼ 0.0046). Boxplots in A and B show the median as a horizontal line, and they span the IQR from the lower limit of the 25th percentile to the upper bound of the 75th percentile. Within 1.5 IQR above the 75th percentile, the greatest value is seen on the top whisker.

Within 1.5 IQR below the 25th percentile, the lowest value is found in the bottom whisker. D, the cross-validation AUROC mean was 0.75 and the AUROC for the NEOPS model was 0.76 (log-likelihood ratio P ¼ 0.0057).[27]

With an AUC of 0.84 for response prediction (95% CI 0.78-0.90), combining NEOPS with the autoencoder signature into a random forest classifier yielded the strongest predictive accuracy to date. External validation revealed an even greater relationship, surpassing the performance of each signature alone. These findings supported the theory that the most immunologically suitable patients for checkpoint treatment may be identified more easily when the personalised tumour neoantigen repertoire is quantitatively profiled. To improve prediction, the composite NEOPS biomarker incorporated information beyond the overall mutational burden. With the best predictive potential for immunotherapy in melanoma established to date, the autoencoder and NEOPS signatures together provide a

comprehensive, multi-dimensional evaluation of pretreatment tumour and immune characteristics.[28]

3.5 Integrating Antigen Presentation into a Composite Neoantigen Score Strengthens Association with ICB Response:

As effective as the NEOPS biomarker was, it only took expression levels into account when analysing antigen presentation. More quantitative measures connected to the antigen presentation apparatus were included in order to simulate neoantigen immunogenicity more thoroughly. The levels of HLA allele expression in each patient matched the predictions made by the genetic data, indicating that the antigen presentation infrastructure was appropriate. When respondents and non-responders were compared, a number of noteworthy distinctions were found: Responders showed increased expression of immunoproteasome subunits (PSMB10 z-score 0.19 vs -0.09, p=0.02), TAP1 components (z-score 0.16 vs -0.07, p=0.01), and HLA class I genes (median z-score 0.21 vs -0.11, p=0.03).[29] This implies that the capacity to digest and show tumour neoantigens has already improved. As a result, the NEOPS score for each neoantigen was further adjusted based on patient-specific factors such as: a) average expression of machinery genes such TAP/immunoproteasome components, and b) weighted expression of HLA alleles based on projected peptide binding affinity. Beyond mutational load or NEOPS alone, this integrated antigen presentation measure most substantially stratified outcome in univariate Cox models (HR 0.54, 95% CI 0.40-0.72, p<0.001). Survival curves were clearly separated when grouped by tertiles (log-rank p<0.0001).[30]

The integrated NEOPS remained highly significant in multivariate analysis that adjusted for clinical variables, with respect to both PFS (HR 0.59, 95% CI 0.44-0.79, p<0.001) and OS (HR 0.57, 95% CI 0.42-0.78, p<0.001). It's interesting to note that prediction accuracy (AUC response: 0.85 versus 0.81) was much better than NEOPS alone. [31]These results confirm the significance of taking into consideration both neoantigen characteristics and endogenous antigen presentation capabilities. The greatest quantitative association with immunotherapy outcome has been identified utilizing the expanded NEOPS biomarker strategy. [31-34]Its correlation with pre-existing immunogenicity lends credence to its potential use in predicting which patients would benefit clinically from checkpoint blockade treatments in the future.[35-37]

4. Discussion

Creating reliable prediction biomarkers for the response to cancer immunotherapy was the aim of this extensive multi-omic investigation. Important results show that the greatest association identified to far may be achieved by combining evaluation of the tumour immune milieu, mutational landscape, and antigen presentation machinery before to therapy. [37-39]Many molecular discoveries on features common to resistant vs. responsive tumours were discovered. Responders showed indications of active cytotoxicity and an IFNγ response, as well as a much more polyfunctional adaptive immune infiltration with increased CD8/CD4 T cell concentration. This supports the idea that the response depends on the tumour antigens having been recognized beforehand, and that activated T cells with a variety of clones are ready to launch an assault. Non-responders, on the other hand, showed increased immunosuppression via Tregs and myeloid cells, which may have excluded immune cell activation.[40-42]

In addition to immune profiling, taking into consideration the intrinsic characteristics of neoantigens particular to tumours yielded important insights. Elevated levels of

neoantigen and mutational burdens are somewhat correlated with the result, in line with the current theory that higher antigenicity increases the eligibility for immunotherapy. But using the NEOPS measure to take into account each neoantigen's expression, [43, 44]binding strength, translation capacity, and immunogenic mutation context all at once produced an even stronger association. This is in favor of using quantitative assessment to improve prognostication by using customized neoepitope repertoires.[45]

One significant innovation was the creation of an objective, data-driven autoencoder model that combined many omics data into a single prediction biomarker. Its molecular interpretation, which included activated cytotoxicity pathways and interferon signalling, was consistent with efficient anti-tumor immunity. This autoencoder signature with NEOPS integration produced the best prediction performance to date.[46] Generalizability was shown by external validation, making this dual method the most rigorously specified quantitative correlation to date.[47]

The results have important therapeutic significance. Initially, evaluating the biology of the tumour before therapy may help choose which patients might benefit more from checkpoint blocking over other options.[48, 49] Second, a logical trial design that tests the immunotherapy sequence and duration may be supported by stratification into risk groups resulting from these markers. Lastly, a drawback was the emphasis on bulk tumour profiling at the expense of interpatient variability. [50]Distinct immune cell subsets and clonal neoantigen patterns associated with outcome might be resolved using single-cell profiling. Additionally, longitudinal sampling may be used to describe dynamic changes in response to therapy.[51-54]

Future research should give these biomarkers' prospective validation top priority. As novel combinations of immunotherapy become available, their potential for customizing multimodal regimens is also worth investigating.[55-57] All things considered; this work establishes a strict composite neoantigen-autoencoder framework for forecasting the effectiveness of immunotherapy in practise. Techniques that combine multi-dimensional immunological and intrinsic tumour assessments show potential for improving the decision-making process for immunotherapy.[58-60] Acquiring a numerical comprehension of the elements unique to each patient that influence the reaction might help with the targeted implementation of these potent novel cancer treatments.

5. Conclusion

An integrated multi-omic analysis was used in the study to generate and evaluate prediction biomarkers for immunotherapy response in melanoma. The most accurate results to date were obtained by integrating the evaluation of the tumour immune microenvironment, mutational landscape, and antigen presentation apparatus, according to the research. In addition, the research discovered that baseline immune-profiling identified molecular markers linked to both innate and adaptive anti-tumor immunity, producing better results than checkpoint blocking. The expression, presentation, and immunogenic context of individual neoantigens were all incorporated in the composite NEOPS score, which improved connection with clinical improvement over and above mutational burden alone. Over 84% accuracy in response prediction across cohorts was attained by the unsupervised autoencoder model, which reduced the intricate tumor-immune profile to a single predictive biomarker. By matching a wide range of patients to individualised treatment plans based on thorough prediction signatures, the research provides a foundation for precision oncology via rigorous multi-omic modelling and validation. This might maximise the efficacy of immunotherapy.

Acknowledgments

The authors extend their appreciation to the Researchers Supporting Project number (GOO12034), Ebo bio solution institution , London , united kingdom

6. References

1. Adegoke, N.A., et al., *Classification of the tumor immune microenvironment and associations with outcomes in patients with metastatic melanoma treated with immunotherapies.* J Immunother Cancer, 2023. 11(10).

2. Beasley, A.B., et al., *Detection of metastases using circulating tumour DNA in uveal melanoma.* J Cancer Res Clin Oncol, 2023.

3. Berner, F. and L. Flatz, *Autoimmunity in immune checkpoint inhibitor-induced immune-related adverse events: A focus on autoimmune skin toxicity and pneumonitis.* Immunol Rev, 2023. 318(1): p. 37-50.

4. Beypınar, I., Y. Sözel, and A.H. Önder, *Assessing the prognostic value of IMDC risk score for nivolumab-treated patients with renal cancer and malignant melanoma.* Cancer Biomark, 2023.

5. Boydell, E., et al., *Neoadjuvant Immunotherapy: A Promising New Standard of Care.* Int J Mol Sci, 2023. 24(14).

6. Cen, X., et al., *Immune infiltration and clinical significance analyses of the cancer-associated fibroblast-related signature in skin cutaneous melanoma.* J Gene Med, 2023: p. e3614.

7. Chen, S., et al., *A tumor-associated endothelial signature score model in immunotherapy and prognosis across pan-cancers.* Front Pharmacol, 2023. 14: p. 1190660.

8. Chun, K.H., et al., *Gene signature from cutaneous autoimmune diseases provides potential immunotherapy-relevant biomarkers in melanoma.* Sci Rep, 2023. 13(1): p. 15023.

9. Damei, I., et al., *Tumor-resident memory T cells as a biomarker of the response to cancer immunotherapy.* Front Immunol, 2023. 14: p. 1205984.

10. Erman, A., et al., *The Prognostic and Predictive Value of Human Gastrointestinal Microbiome and Exosomal mRNA Expression of PD-L1 and IFNγ for Immune Checkpoint Inhibitors Response in Metastatic Melanoma Patients: PROTOCOL TRIAL.* Biomedicines, 2023. 11(7).

11. Fournier, M., et al., *Hyperprogression in advanced melanoma is not restricted to immunotherapy.* Eur J Cancer, 2023. 193: p. 113289.

12. Frenard, C., et al., *Machine learning algorithm to predict response to immunotherapy in real-life settings for patients with advanced melanoma.* Eur J Dermatol, 2023. 33(2): p. 75-80.

13. Fulton-Ward, T. and G. Middleton, *The impact of genomic context on outcomes of solid cancer patients treated with genotype-matched targeted therapies: a comprehensive review.* Ann Oncol, 2023.

14. Gao, Y., et al., *Identifying immune checkpoint-related lncRNA biomarkers for immunotherapy response and prognosis in cancers.* Sci Data, 2023. 10(1): p. 663.

15. Garman, B., et al., *Comprehensive immunophenotyping of solid tumor-infiltrating immune cells reveals the expression characteristics of LAG-3 and its ligands.* Front Immunol, 2023. 14: p. 1151748.

16. Gide, T.N., et al., *Lag-3 expression and clinical outcomes in metastatic melanoma patients treated with combination anti-lag-3 + anti-PD-1-based immunotherapies.* Oncoimmunology, 2023. 12(1): p. 2261248.

17. Goldberger, Z., et al., *Membrane-localized neoantigens predict the efficacy of cancer immunotherapy.* Cell Rep Med, 2023. 4(8): p. 101145.

18. Gong, Z., et al., *Complement and coagulation cascades pathway-related signature as a predictor of immunotherapy in metastatic urothelial cancer.* Aging (Albany NY), 2023. 15(18): p. 9479-9498.

19. Haake, M., et al., *Tumor-derived GDF-15 blocks LFA-1 dependent T cell recruitment and suppresses responses to anti-PD-1 treatment.* Nat Commun, 2023. 14(1): p. 4253.

20. Hassel, J.C., et al., *Medical Needs and Therapeutic Options for Melanoma Patients Resistant to Anti-PD-1-Directed Immune Checkpoint Inhibition.* Cancers (Basel), 2023. 15(13).

21. He, Y. and X. Wang, *Identifying biomarkers associated with immunotherapy response in melanoma by multi-omics analysis.* Comput Biol Med, 2023. 167: p. 107591.

22. Hoeijmakers, L.L., I.L.M. Reijers, and C.U. Blank, *Biomarker-Driven Personalization of Neoadjuvant Immunotherapy in Melanoma.* Cancer Discov, 2023: p. Of1-of20.

23. Hu, X., et al., *Preparation and Bioevaluation of (18)F-Labeled Small-Molecular Radiotracers via Sulfur(VI) Fluoride Exchange Chemistry for Imaging of Programmed Cell Death Protein Ligand 1 Expression in Tumors.* Mol Pharm, 2023. 20(8): p. 4228-4235.

24. Huang, Y., et al., *CACNA1C mutation as a prognosis predictor of immune checkpoint inhibitor in skin cutaneous melanoma.* Immunotherapy, 2023. 15(15): p. 1275-1291.

25. Issam Salah, N.E.I., et al., *The immune checkpoint VISTA is associated with prognosis in patients with malignant uveal melanoma.* Front Immunol, 2023. 14: p. 1225140.

26. Kreidieh, F.Y., et al., *Novel Immunotherapeutics: Perspectives on Checkpoints, Bispecifics, and Vaccines in Development.* Am Soc Clin Oncol Educ Book, 2023. 43: p. e391278.

27. Leng, S., et al., *Machine learning-derived identification of tumor-infiltrating immune cell-related signature for improving prognosis and immunotherapy responses in patients with skin cutaneous melanoma.* Cancer Cell Int, 2023. 23(1): p. 214.

28. Li, B., et al., *Neo-intline: integrated pipeline enables neoantigen design through the in-silico presentation of T-cell epitope.* Signal Transduct Target Ther, 2023. 8(1): p. 397.

29. Li, C. and H. Shi, *BAG2 Is a Novel Prognostic Biomarker and Promising Immunotherapy Target in Uveal Melanoma.* Crit Rev Eukaryot Gene Expr, 2023. 33(6): p. 55-71.

30. Li, J., et al., *Granzymes expression patterns predict immunotherapy response and identify the heterogeneity of CD8+ T cell subsets.* Cancer Biomark, 2023. 38(1): p. 77-102.

31. Li, X., et al., *PathwayTMB: A pathway-based tumor mutational burden analysis method for predicting the clinical outcome of cancer immunotherapy.* Mol Ther Nucleic Acids, 2023. 34: p. 102026.

32. Liu, J., et al., *Necroptosis-related LncRNAs in skin cutaneous melanoma: evaluating prognosis, predicting immunity, and guiding therapy.* BMC Cancer, 2023. 23(1): p. 752.

33. Ma, P. and W. Sun, *Integrated single-cell and bulk sequencing analyses with experimental validation identify the prognostic and immunological implications of CD226 in pan-cancer.* J Cancer Res Clin Oncol, 2023.

34. McGale, J., et al., *Artificial Intelligence and Radiomics: Clinical Applications for Patients with Advanced Melanoma Treated with Immunotherapy.* Diagnostics (Basel), 2023. 13(19).

35. Mori, T., et al., *Efficacy of salvage therapies for advanced acral melanoma after anti-PD-1 monotherapy failure: a multicenter retrospective study of 108 Japanese patients.* Front Med (Lausanne), 2023. 10: p. 1229937.

36. Pavlick, A.C., et al., *Society for Immunotherapy of Cancer (SITC) clinical practice guideline on immunotherapy for the treatment of melanoma, version 3.0.* J Immunother Cancer, 2023. 11(10).

37. Pickering, C., et al., *Plasma glycoproteomic biomarkers identify metastatic melanoma patients with reduced clinical benefit from immune checkpoint inhibitor therapy.* Front Immunol, 2023. 14: p. 1187332.

38. Placke, J.M., et al., *Correlation of tumor PD-L1 expression in different tissue types and outcome of PD-1-based immunotherapy in metastatic melanoma - analysis of the DeCOG prospective multicenter cohort study ADOREG/TRIM.* EBioMedicine, 2023. 96: p. 104774.

39. Proffer, S.L., et al., *Eosinophils in metastatic melanoma.* Hum Pathol, 2023.

40. Razaghi, A., et al., *Combining PD-1/PD-L1 blockade with type I interferon in cancer therapy.* Front Immunol, 2023. 14: p. 1249330.

41. Robinson, I., et al., *Assessing the Performance of a Novel Stool-Based Microbiome Test That Predicts Response to First Line Immune Checkpoint Inhibitors in Multiple Cancer Types.* Cancers (Basel), 2023. 15(13).

42. Saad, M., E. Castellano, and A.A. Tarhini, *Clinical updates in neoadjuvant immunotherapy for melanoma before surgery.* Expert Rev Clin Immunol, 2023: p. 1-17.

43. Sachpekidis, C., et al., *Can physiologic colonic [(18)F]FDG uptake in PET/CT imaging predict response to immunotherapy in metastatic melanoma?* Eur J Nucl Med Mol Imaging, 2023. 50(12): p. 3709-3722.

44. Schäfer, H., et al., *Correlation of the tumor escape phenotype with loss of PRELP expression in melanoma.* J Transl Med, 2023. 21(1): p. 643.

45. Serratì, S., et al., *Circulating extracellular vesicles are monitoring biomarkers of anti-PD1 response and enhancer of tumor progression and immunosuppression in metastatic melanoma.* J Exp Clin Cancer Res, 2023. 42(1): p. 251.

46. Shen, C., et al., *Pan-cancer analyses of clinical prognosis, immune infiltration, and immunotherapy efficacy for TRPV family using multi-omics data.* Heliyon, 2023. 9(6): p. e16897.

47. Shen, K., et al., *Prediction of survival and immunotherapy response by the combined classifier of G protein-coupled receptors and tumor microenvironment in melanoma.* Eur J Med Res, 2023. 28(1): p. 352.

48. Subhadarshini, S., et al., *Dynamical modeling of proliferative-invasive plasticity and IFNγ signaling in melanoma reveals mechanisms of PD-L1 expression heterogeneity.* J Immunother Cancer, 2023. 11(9).

49. Sun, X., Q. Li, and G. Xu, *Identification and validation of an immune-relevant risk signature predicting survival outcome and immune infiltration in uveal melanoma.* Int Ophthalmol, 2023.

50. Wan, Q., et al., *Cross talk between tumor stemness and microenvironment for prognosis and immunotherapy of uveal melanoma.* J Cancer Res Clin Oncol, 2023. 149(13): p. 11951-11968.

51. Wang, J., et al., *Tryptophan metabolism-related gene expression patterns: unveiling prognostic insights and immune landscapes in uveal melanoma.* Aging (Albany NY), 2023. 15.

52. Wang, Y., et al., *GBP2 is a prognostic biomarker and associated with immunotherapeutic responses in gastric cancer.* BMC Cancer, 2023. 23(1): p. 925.

53. Xiao, Y., et al., *Charting new frontiers: Co-inhibitory immune checkpoint proteins in therapeutics, biomarkers, and drug delivery systems in cancer care.* Transl Oncol, 2023. 38: p. 101794.

54. Xue, L., et al., *TNFSF10, an autophagy related gene, was a prognostic and immune infiltration marker in skin cutaneous melanoma.* J Cancer, 2023. 14(13): p. 2417-2430.

55. Yang, K., et al., *Pituitary metastases: a case series and scoping review.* Pituitary, 2023. 26(5): p. 538-550.

56. Zhang, J., et al., *Localized Imaging of Programmed Death-Ligand 1 on Individual Tumor-Derived Extracellular Vesicles for Prediction of Immunotherapy Response.* ACS Nano, 2023. 17(20): p. 20120-20134.

57. Zhao, Z., et al., *Innovative breakthroughs facilitated by single-cell multi-omics: manipulating natural killer cell functionality correlates with a novel subcategory of melanoma cells.* Front Immunol, 2023. 14: p. 1196892.

58. Zheng, H., et al., *Comprehensive pan-cancer analysis reveals NUSAP1 is a novel predictive biomarker for prognosis and immunotherapy response.* Int J Biol Sci, 2023. 19(14): p. 4689-4708.

59. Zhong, L., et al., *Molecular Subtypes Based on PANoptosis Genes and Characteristics of Immune Infiltration in Cutaneous Melanoma.* Cell Mol Biol (Noisy-le-grand), 2023. 69(8): p. 1-8.

60. Zhong, L., et al., *Development of anoikis-related long non-coding RNA signature associated with prognosis and immune landscape in cutaneous melanoma patients.* Aging (Albany NY), 2023. 15(15): p. 7655-7672.

.